Journal of Cleaner Production xxx (xxxx) xxx

Contents lists available at ScienceDirect

Journal of Cleaner Production

journal homepage: www.elsevier.com/locate/jclepro

Prediction short-term photovoltaic power using improved chicken swarm optimizer - Extreme learning machine model

Zhi-Feng Liu [a, b], Ling-Ling Li [a, b], Ming-Lang Tseng [c, d, *], Ming K. Lim [e]

[a] State Key Laboratory of Reliability and Intelligence of Electrical Equipment, Hebei University of Technology, Tianjin, 300130, China
[b] Key Laboratory of Electromagnetic Field and Electrical Apparatus Reliability of Hebei Province, Hebei University of Technology, Tianjin, 300130, China
[c] Institute of Innovation and Circular Economy, Asia University, Taichung, Taiwan
[d] Department of Medical Research, China Medical University, Taichung, Taiwan
[e] Coventry University, United Kingdom

ARTICLE INFO

Article history:
Received 7 August 2019
Received in revised form
8 November 2019
Accepted 11 November 2019
Available online xxx

Handling Editor: Bin Chen

Keywords:
Photovoltaic power generation
Extreme learning machine
Intelligent optimizer
Power prediction
Model-driven method

ABSTRACT

Photovoltaic power generation is greatly affected by weather conditions while the photovoltaic power has a certain negative impact on the power grid. The power sector takes certain measures to abandon photovoltaic power generation, thus limiting the development of clean energy power generation. This study is to propose an accurate short-term photovoltaic power prediction method. A new short-term photovoltaic power output prediction model is proposed Based on extreme learning machine and intelligent optimizer. Firstly, the input of the model is determined by correlation coefficient method. Then the chicken swarm optimizer is improved to strengthen the convergence. Secondly, the improved chicken swarm optimizer is used to optimize the weights and the extreme learning machine thresholds to improve the prediction effect. Finally, the improved chicken swarm optimizer extreme learning machine model is used to predict the photovoltaic power under different weather conditions. The testing results show that the average mean absolute percentage error and root mean square error of improved chicken swarm optimizer - extreme learning machine model are 5.54% and 3.08%. The proposed method is of great significance for the economic dispatch of power systems and the development of clean energy.

1. Introduction

China's energy demand has grown rapidly as a big energy consuming country. A large amount of fossil fuel consumption has brought serious environmental problems to China, such as China facing serious smog problems (Zhang et al., 2019; Xiong et al., 2019). This is imperative to develop clean energy in order to solve this thorny problem. Especially, photovoltaic (PV) energy power generation has received the attention of the Chinese government with the continuous advancement of technology. To this end, the Chinese government has formulated relevant policies to promote the development of clean energy power generation. According to the 13th Five-Year development plan of clean energy made by China energy administration, the power plant will maintain an annual average installed capacity of 20–23 GW, which is not subject to the index (Guo et al., 2019).

Traditional power grid scheduling is based on reliable power supply and predictable load. The reliability of power grid operation can be improved by regulating the power supply side and the power consumption side (Li et al., 2018). However, PV power generation is random, intermittent and fluctuant under the influence of weather and environment (Seyedmahmoudian et al., 2018; Monfared et al., 2019; Sanchez-Sutil et al., 2019). These characteristics of PV power generation will have a negative impact on the stable operation of power system. When large-scale PV power is integrated into the grid, the generation side will be uncontrollable, which will have a negative impact on the grid's power generation plan (Menezes et al., 2018). At this time, the grid will adopt "PV power curtailment" measure to reduce the impact of PV power generation on the grid, thus limiting the development of clean energy power generation (Hernandez et al., 2018). The more accurate the PV power forecasting is, the less PV power limitation will occur in the grid, which greatly improves the development and utilization of clean energy, thereby reducing the economic losses to

* Corresponding author. Institute of Innovation and Circular Economy, Asia University, Taichung, Taiwan.
E-mail addresses: tjliuzhifeng@126.com (Z.-F. Liu), lilinglinglaoshi@126.com (L.-L. Li), tsengminglang@gmail.com (M.-L. Tseng), ming.lim@cqu.edu.cn (M.K. Lim).

https://doi.org/10.1016/j.jclepro.2019.119272
0959-6526/

Nomenclature variables

P	Connection weight between hidden layer and input layer
D	Connection weight between hidden layer and input layer
M	Samples
A	Input quantity
B	Output quantity
$X(\bullet)$	Activation function
O	Network output
K	Hidden layer output
K^{+}	Moore-Penrose generalized inverse
ε	Infinitesimal
BL	Learning coefficient
$randm$	Random number between 0 and 1
GL	Random number between 0 and 2
Z	Position
Cip	Cosine inertia weight
z	Pre-mutation particle
λ	Cauchy mutation operator
z^{*}	Mutated particle
R^2	Decision coefficient

Acronyms list

PV	Photovoltaic
SVM	Support vector machine
AI	Artificial intelligence
ANN	Artificial neural network
AR	Autoregressive
MA	Moving average
ARMA	Autoregressive moving average
DBN	Deep belief network
BP	Back propagation
CSO	Chicken swarm optimizer
ICSO	Improved chicken swarm optimizer
GPR	Gaussian process regression
GA	Genetic optimizer
SVR	Support vector regression
RMSE	Root mean square error
ELM	Extreme learning machine
SLFN	Single-hidden layer feed forward neural network
PSO	Particle swarm optimizer
WOA	Whale optimizer
MAPE	Mean absolute percentage error

PV owners caused by power limitation, and increasing the return on investment of PV power plants. Therefore, it is necessary to accurately predict PV power generation, and it has important value to develop the clean energy power generation technology.

In terms of PV power prediction, the specific time scale, the PV power forecasting can be divided into four types: medium-term and long-term prediction (days or weeks), short-term prediction (hours or one day), ultra-short-term prediction (1 min or a few minutes). Ultra-short-term PV power prediction is mainly used for real-time dispatching of power grid; short-term PV power forecasting is mainly used to assist the dispatch sector to formulate daily generation plans and economic dispatching plans; medium and long-term PV power output forecasting is mainly used for the maintenance of PV power field and operation management of PV power plants (Han et al., 2019a,b; Lin et al., 2018; Izgi et al., 2012). Because short-term PV power prediction is of great significance for the power sector to arrange reasonable daily power generation plans, achieve efficient economic dispatch and promote the development and utilization of clean energy, it has become a current research hotspot.

At present, the main research methods for PV power prediction can be divided into two types: prediction methods based on statistical analysis models and prediction methods based on artificial intelligence (AI) models (Raza et al., 2016). The two methods can achieve the prediction of PV power, but the prediction principles of the two methods are very different. The prediction method based on statistical analysis model can forecast the next stage of PV power generation according to historical data of PV power generation. There are three kinds of statistical regression models: autoregressive moving average (ARMA) model, autoregressive (AR) model and moving average (MA) model (Xie et al., 2018, Wang et al., 2018a,b). Data-driven AI model is trained with historical data, and then the trained model is used to predict PV power. The main AI models commonly used in PV power prediction are artificial neural network (ANN), support vector machine (SVM), extreme learning machine (ELM) (Lin and Pai, 2016; Nespoli et al., 2019; Zhu et al., 2017).

Because PV power is greatly influenced by climate conditions, PV power output has strong non-linearity. Statistical analysis model uses historical data to further predict the development trend of power output. The statistical analysis model has a large deviation while the PV power changes greatly. Compared with statistical analysis model, AI model has stronger ability of non-linear mapping. For example, SVM, ELM and other models have been applied to the field of PV power prediction. Among them, the ELM model has been widely used in the forecasting field due to its strong generalization ability and nonlinear prediction ability. Because the super parameters (weight values and threshold values) in ELM model have a great influence on the prediction results, how to optimize the super parameters of ELM model is the key problem. Therefore, it is necessary to propose an appropriate optimizer. In this study, improved chicken swarm optimizer (ICSO) is combined with ELM to optimize the super parameters of ELM. ICSO-ELM model is proposed for PV power prediction. ICSO-ELM model is used to predict the PV power under cloudy, sunny and rainy weather conditions respectively. At the same time, compared with many existing models, the superiority of the proposed model is verified. The contributions of this study are as follows:

(1) The CSO optimizer has been improved to propose the ICSO optimizer.
(2) The input of the model is determined by correlation coefficient method.
(3) The ICSO-ELM model is proposed to forecast the short-term PV power under three specific weather conditions.
(4) Accurate PV forecasting can effectively help the power grid dispatching department to make various power dispatch schedules and promote the development and utilization of clean energy.

2. Literature review

In practical applications, when PV power affects the stable operation of the system, the power sector will take “PV power curtailment” measures to control the impact of PV power on the

Please cite this article as: Liu, Z.-F et al., Prediction short-term photovoltaic power using improved chicken swarm optimizer - Extreme learning machine model, Journal of Cleaner Production, https://doi.org/10.1016/j.jclepro.2019.119272

stability of power grid, which will limit the development of clean energy. Through short-term PV power prediction, the efficient economic dispatching plan and daily generation plan for the power sector are formulated to reduce the restrictive measures of PV power generation, thus promoting the development of clean energy. Therefore, short-term PV power prediction is very necessary and is of great significance to the development and utilization of clean energy. At present, scholars have proposed many short-term photovoltaic power forecasting methods. Generally, these methods can be divided into three kinds: time series prediction model, artificial intelligence (AI) model and hybrid model based on time series and AI model. Based on historical meteorological data and power data, the time series model establishes the mapping relationship between them, and predicts power by the mapping relationship. The nonlinear fitting ability of the time series model is poor, and when the prediction period is longer, there will be greater prediction error. Therefore, the model is suitable for ultra-short-term PV power prediction. Autoregressive (AR) model and autoregressive moving average (ARMA) model are two common time series models. Bacher et al. (2009) presented an online short-term PV forecasting method. Firstly, the PV power was normalized. Secondly, the adaptive linear time series model was used to predict the PV power. Since traditional ARMA model cannot consider climate information, climate information has an impact on improving model prediction accuracy. To this end, Li et al. (2014) previously proposed a generalized ARMA model that took into account climate information and used these climate information as input to the model.

Compared with the time series model, more and more scholars begin to pay attention to AI model and hybrid model. Based on the deep belief network (DBN) and the ARMA model, Xie et al. (2018) proposed a hybrid model to forecast short-term PV power. Firstly, time series were decomposed into high frequency components and low frequency components. Then DBN model was used to predict the high frequency components, ARMA model was used to predict the decomposed low frequency components, and finally the predicted components were synthesized into the final results. Li et al. (2019a,b), Bouzerdoum et al. (2013), Eseye et al. (2018) and VanDeventer et al. (2019) used SVM to predict short-term PV power, and optimizer was used to optimize the super parameters of SVM to reduce the influence of super parameters on the prediction effects. Since the SVM solves the support vector by means of quadratic programming, when the number of samples is large, the training time of the SVM is long. Artificial neural network (ANN) is widely used in short-term PV forecasting because of its strong fault tolerance and strong non-linear mapping ability. Based on ANN and analog integration, Cervone et al. (2017) proposed a combined method to forecast PV power. Dolara et al. (2015) proposed a combined model based on ANN and clear sky curve of PV power station. ELM is developed based on feedforward neuron network (FNN). The ELM model does not need to adjust the weight and threshold in the training process. It has the characteristics of fast training speed and strong generalization ability, and has a good application prospect (Huang et al., 2006; Guner et al., 2019).

The ELM model can effectively solve complex nonlinear regression problems, so it is used for irradiance prediction and PV power output prediction. Han et al. (2019a,b) proposed a prediction method based on ELM model considering the characteristics of PV power fluctuation. Firstly, the seasonal characteristics of PV output power fluctuating with time were analyzed. Then, the PV output power was predicted by the ELM model. Hossain et al. (2017) used the extreme learning machine (ELM) to predict the short-term PV power. The test results show that compared with support vector regression (SVR) and ANN, ELM model has higher prediction accuracy. Liu et al. (2018) and Ni et al. (2017) combined ELM model with other methods to predict short-term PV power. This combination method can avoid the defects of a single model, which is relatively complex and has high computational cost. The core of ELM is how to select hyper-parameters, which will affect the prediction accuracy of ELM model. At present, the main method adopted by scholars is to optimize super parameters through intelligent optimizer. For example, genetic optimizer (GA), whale optimizer (WOA) and particle swarm optimizer (PSO) are used to optimize the super parameters of ELM model (Xue et al., 2018; Li et al., 2019a,b; Wang et al., 2019). The improved chicken swarm optimizer (ICSO) is used to optimize the super parameters of the ELM model to improve the prediction effect. At present, the proposed models have achieved good prediction results. The R^2 of the SARIMA-SVM model proposed by Bouzerdoum et al. (2013) is 99.08%; the average MAPE of the HIMVO-SVM model is 5.12% (Li et al., 2019a,b); the RMSE of the GA-SVM model is 11.22% (VanDeventer et al., 2019); the MAPE of the WT-PSO-SVM model proposed by Eseye et al., (2018) is 4.2%; the average RMSE, MAPE and R^2 of ICSO-ELM model are 5.54%, 3.08% and 99.32% respectively for three different weather conditions. Compared with the proposed models, the ICSO-ELM model has advantages in prediction effect and fitting accuracy.

3. Prediction model of PV power

3.1. The principle of extreme learning machine

The single-hidden layer feed forward neural network (SLFN) has the characteristics of simple structure and fast convergence. SLFN is used in prediction, classification, pattern recognition and other fields. However, SLFN has the disadvantages of slow training speed, sensitivity to learning rate. The ELM is a new type of SLFN. The connection weight between the hidden layer and the input layer is randomly determined. The threshold of hidden layer neurons is also randomly determined (Hossain et al., 2017).

ELM is faster and more generalizable than other predictive models (Li et al., 2019a,b; Liu et al., 2018). The SLFN consists of three layers. And three layers are connected by neurons. The input layer has e neurons, the output layer has t neurons and the hidden layer has v neurons. The threshold value of hidden layer neurons is $\mathbf{q} = [q_1, q_2, \ldots, q_v]^T$. The connection weight between hidden layer and input layer is **P**, and the connection weight between output layer and hidden layer is **D**.

$$\mathbf{P} = \begin{bmatrix} p_{11} & p_{12} & \cdots & p_{1e} \\ p_{21} & p_{22} & \cdots & p_{2e} \\ & \vdots & \vdots & \\ p_{v1} & p_{v2} & \cdots & p_{ve} \end{bmatrix}_{v\times e} \quad \mathbf{D} = \begin{bmatrix} d_{11} & d_{12} & \cdots & d_{1t} \\ d_{21} & d_{22} & \cdots & d_{2t} \\ & \vdots & \vdots & \\ d_{v1} & d_{v2} & \cdots & d_{vt} \end{bmatrix}_{v\times t} \tag{1}$$

Supposed there are M samples. **A** represents the input quantity and **B** represents the output quantity.

$$\mathbf{A} = \begin{bmatrix} a_{11} & a_{12} & \cdots & a_{1M} \\ a_{21} & a_{22} & \cdots & a_{2M} \\ & \vdots & \vdots & \\ a_{e1} & a_{e2} & \cdots & a_{eM} \end{bmatrix}_{e\times M} \quad \mathbf{B} = \begin{bmatrix} b_{11} & b_{12} & \cdots & b_{1M} \\ b_{21} & b_{22} & \cdots & b_{2M} \\ & \vdots & \vdots & \\ b_{t1} & b_{t2} & \cdots & b_{tM} \end{bmatrix}_{t\times M} \tag{2}$$

$X(\cdot)$ is the activation function and **O** is the network output.

Please cite this article as: Liu, Z.-F et al., Prediction short-term photovoltaic power using improved chicken swarm optimizer - Extreme learning machine model, Journal of Cleaner Production, https://doi.org/10.1016/j.jclepro.2019.119272

$$\mathbf{O} = [\mathbf{o}_1, \mathbf{o}_2, \cdots, \mathbf{o}_M]_{t\times M}$$

$$where\ \mathbf{o}_j = \begin{bmatrix} o_{1j} \\ o_{2j} \\ \vdots \\ o_{tj} \end{bmatrix} = \begin{bmatrix} \sum_{i=1}^{v} d_{i1} X(\mathbf{p}_i \mathbf{a}_j + q_i) \\ \sum_{i=1}^{v} d_{i2} X(\mathbf{p}_i \mathbf{a}_j + q_i) \\ \vdots \\ \sum_{i=1}^{v} d_{it} X(\mathbf{p}_i \mathbf{a}_j + q_i) \end{bmatrix}_{t\times 1} \quad (j = 1, 2, \cdots, M) \tag{3}$$

The hidden layer activation function uses the sigmoid function, and its calculation equation is as follows.

$$X(a) = \frac{1}{1 + e^{-a}} \tag{4}$$

Simplify equation (4) to $\mathbf{KD} = \mathbf{O}^T$.

Where $\mathbf{K}$ is the hidden layer output. The equation is as follows.

$$\mathbf{K} = \begin{bmatrix} X(\mathbf{p}_1\mathbf{a}_1 + q_1) & X(\mathbf{p}_2\mathbf{a}_1 + q_2) & \cdots & X(\mathbf{p}_v\mathbf{a}_1 + q_v) \\ X(\mathbf{p}_1\mathbf{a}_2 + q_1) & X(\mathbf{p}_2\mathbf{a}_2 + q_2) & \cdots & X(\mathbf{p}_v\mathbf{a}_2 + q_v) \\ & & \vdots & \\ X(\mathbf{p}_1\mathbf{a}_M + q_1) & X(\mathbf{p}_2\mathbf{a}_M + q_2) & \cdots & X(\mathbf{p}_v\mathbf{a}_M + q_v) \end{bmatrix}_{M\times v} \tag{5}$$

As $X(\cdot)$ is infinitely differentiable, $\mathbf{p}$ and $\mathbf{d}$ are arbitrarily selected, and the values do not change during the training.

$$\min_D \left\| \mathbf{KD} - \mathbf{O}^T \right\| \tag{6}$$

The solution of $\mathbf{D}$ is as follows.

$$\hat{\mathbf{D}} = \mathbf{K}^{+}\mathbf{O}^T \tag{7}$$

where $\mathbf{K}^+$ is the Moore-Penrose generalized inverse of $\mathbf{K}$.

3.2. Chicken swarm optimizer (CSO)

Meng et al. (2014) proposed the CSO optimizer. The CSO optimizer is a group intelligent optimizer that simulates the hierarchical system and the foraging behavior of the chicken swarm. The optimizer divides chickens into groups. Every group includes a cock, several hens and a few chicks. In the CSO optimizer, the following rules are used to simulate the behaviors of the flock (Shi et al., 2018).

(1) There are several subpopulations in the chicken population. Each subpopulation includes a cock, multiple hens and chicks. Cocks have the strongest foraging ability and dominate the flock. The hen's foraging ability is the second, and the chick's foraging ability is the worst.
(2) The flocks are classified according to fitness values. A few of chickens with good fitness values are selected as cocks and a few of chickens with poor fitness are selected as chicks. The remaining chickens are selected as hens. The hens are arbitrarily added to a subgroup. Chicks and mother hens are randomly selected.
(3) The mother-child relationship and leadership relationship remain unchanged under a specific hierarchy. But as the chicks grow, these states are updated every G time (G is the update time, which is a certain value).
(4) Hens follow the roosters in their group to forage, and can steal food from other chickens. The chicks follow the hens and look for food around the hens.

When solving an optimization problem, the position of each chicken represents a feasible solution. Because each chicken has different foraging capabilities, different chickens have different update strategies. Assuming that the search space of chickens is d, there are N chickens in total. There are N_c chicks, N_h hens and N_r cocks. At time t, $Z_{i,j}^t (j = 1, 2, \cdots, d;\ i = 1, 2, \cdots, N)$ represents the position of the i_{th} chicken in the j_{th} dimension.

The update equation of the i_{th} rooster is as follows.

$$Z_{i,j}^{t+1} = Z_{i,j}^t + Z_{i,j}^t * randn\left(0,\ \sigma^2\right)$$

$$\sigma^2 = \begin{cases} 1 & S_e \geq S_i \\ \exp\left(\dfrac{S_e - S_i}{|S_i + \varepsilon|}\right) & S_e < S_i \end{cases} \tag{8}$$

where $randn(0,\ \sigma^2)$ represents the Gaussian distribution. $S_e (e \in [1,\ N_r],\ i \neq e)$ indicates a cock other than the i_{th} cock. ε is infinitesimal, ensuring that the denominator is not 0.

The update equation of the i_{th} hen is as shown in Equation (9).

$$Z_{i,j}^{t+1} = Z_{i,j}^t + p1 * randm * \left(Z_{r1,j}^t - Z_{i,j}^t\right) + p2 * randm * \left(Z_{r2,j}^t - Z_{i,j}^t\right)$$

$$\begin{cases} p1 = \exp\left(\dfrac{S_i - S_{r1}}{ads(S_i + \varepsilon)}\right) \\ p2 = (S_{r2} - S_i) \end{cases} \tag{9}$$

where *randm* represents a random number between 0 and 1. $r1$ is the cock in the group where the i_{th} hen is located. $r2 (r1 \neq r2)$ is the cock in the other group.

The equation for updating chick particles is as follows.

$$Z_{i,j}^{t+1} = Z_{i,j}^t + GL(i) * \left(Z_{m,j}^t - Z_{i,j}^t\right) \tag{10}$$

where $Z_{m,j}^t$ is the mother chicken followed by the i_{th} chick; *GL* represents a random number between 0 and 2.

3.3. Improved chicken swarm optimizer

The traditional CSO optimizer has poor global search and local search capabilities when dealing with more complex problems. To solve this problem, this study improves the CSO optimizer and strengthens the global and local search capabilities of the CSO optimizer. In the CSO optimizer, the cock dominates the flock and has the strongest foraging ability. When the cock in the flock is caught in a local optimum and causes the whole flock to fall into local optimum. The cosine inertia weight *Cip* is introduced to strengthen the local search ability of cock particles.

The optimal particle learning part is introduced in the chick particle position update equation in order to expand the search range of chick particles. The search range of the flock is gradually narrowing at the later stage of iteration. Cauchy mutation operator is introduced to enhance the diversity of population in the later stage of iteration.

After introducing the cosine inertia weight, the position update equation of the i_{th} cock particle is as follows.

Please cite this article as: Liu, Z.-F et al., Prediction short-term photovoltaic power using improved chicken swarm optimizer - Extreme learning machine model, Journal of Cleaner Production, https://doi.org/10.1016/j.jclepro.2019.119272

$$Z_{i,j}^{t+1} = Cip*Z_{i,j}^{t} + Z_{i,j}^{t}*randn\left(0,\ \sigma^2\right)$$
$$Cip = Cip_{\min} + (Cip_{\max} - Cip_{\min})*\cos\left(\pi*\frac{t}{T}\right) \quad (11)$$

where $Cip_{\min} = 0.3$, $Cip_{\max} = 0.8$.

During the whole iteration process, the cock particles first globally search and then locally search. The local and global search ability of cock particles are improved by cosine inertia weight Cip.

After improvement, the position update equation of the i_{th} chick is as follows.

$$Z_{i,j}^{t+1} = Z_{i,j}^{t} + GL(i)*\left(Z_{m,j}^{t} - Z_{i,j}^{t}\right) + BL(i)*\left(Z_{best,j}^{t} - Z_{i,j}^{t}\right)$$
$$BL(i) = \exp(S_{best} - S_i) \quad (12)$$

where BL is the learning coefficient; S_{best} is the best particle in the flock.

The chick particles not only learn from the hen particles around them, but also learn from the best particle in the flock. The search range of the chick particle can be enlarged by learning from the best particle, which can avoid the chick particle falling into the local optimum to some extent.

In the later stage of population search, the flock is more likely to fall into the local optimal value. Therefore, the current iteration number exceeds 90% of the total number of iterations and the Cauchy mutation operation is introduced. The diversity of chicken flocks can be increased by mutating populations. Cauchy mutation operator has more mutation ability compared with normal distribution, which can expand the search range of population. The calculation process of Cauchy mutation operator is as follows.

$$z^* = z + \lambda*Cauchy(t) \quad (13)$$

where z is the pre-mutation particle; z^* is the mutated particle; $Cauchy(t)$ is the Cauchy distribution random variable; λ controls the variation intensity of the Cauchy mutation operator.

3.4. Establishment of ICSO-ELM prediction model

At present, the commonly used forecasting methods are SVM model, ARMA model and BP model and so on. The SVM model has strong nonlinear mapping ability, but the SVM model is suitable for small samples, so the SVM model is more used to forecast ultra-short-term PV power. The ARMA model is based on statistical regression. When the PV power is greatly affected by weather conditions, the prediction error of the ARMA model is larger. The gradient descent method adopted in BP model leads to slow training speed and sensitivity to the choice of learning rate. Compared with these traditional prediction models, ELM model has faster learning speed and stronger generalization ability.

Improving the prediction accuracy of the short-term PV power prediction model has positive significance for realizing economic dispatch and promoting the development of clean energy generation technology. However, the connection weight D and the threshold q in the ELM are randomly selected. If the values are not properly selected and directly affect the prediction effect of the ELM. Therefore, the optimizer is needed to optimize the super parameters of the ELM model, the performance of the optimizer has a great influence on the prediction accuracy of the ELM model.

Compared with the traditional optimizers, ICSO optimizer has stronger convergence ability and has a greater impact on improving the prediction effect of ELM model. In this study, ICSO is used to optimize D and q. The optimal D and q of ELM are obtained by ICSO optimizer, which improves the prediction accuracy of ELM. The prediction process of ICSO-ELM model is illustrated in Fig. 1 and explained as follows:

(1) Determine PV power output samples.
(2) Normalize sample data.
(3) Initialize parameters of ICSO optimizer.
(4) Update the position of each particle according to the location update strategy.
(5) ICSO optimizer is used to optimize the super parameters of ELM model.
(6) The trained model is used to predict the PV power output.
(7) Evaluate the predictive effect.

4. Influencing attributes of PV power output

4.1. Analysis of PV power output curves in sunny, rainy and cloudy weather

The PV power output is greatly affected by the weather conditions. Different weather conditions have different effects on PV power output. So the PV power output is unstable. The experimental data of this study is from the Desert Knowledge Australia Solar Centre (DKASC). DKASC is a demonstration facility for commercial solar technology in the central region of Australia. The sunny weather power output data of August 14, 2016, the cloudy weather power output data of December 1, 2016 and the rainy weather power output data of August 15, 2016 are selected to plot the PV output power curve. The study period of the PV power historical data is 8:00–17:00, which is counted every 5 min. The amount of sunlight in other periods is small, so it is not in the statistical range.

Fig. 2 indicated the fluctuation of power output curve in sunny weather is smaller than that in rainy weather. In sunny weather, the output power increases with the increase of illumination intensity from 8:00 to 13:00. The PV power output reaches its maximum at about 13:00. After 13:00, the output power decreases with the decrease of illumination intensity as time goes on.

In rainy weather and cloudy weather, the power output curves of PV power generation system do not show a cycle trend. There is no specific law of power output in rainy weather, and the fluctuation of power output curves in rainy and cloudy weather are greater than that in sunny weather.

4.2. The influence of different meteorological elements on PV power output

The radiation intensity, relative humidity, wind speed and temperature affects the PV power output. Because of the influence of these meteorological elements, PV power has the characteristics of instability and intermittence. But each meteorological element has different influence on the PV power output.

This study uses correlation coefficient method to analyze the influence of meteorological elements. The relationship curves between output power and wind speed, temperature, relative humidity and radiation intensity are drawn based on the historical data of April 13, 2016. The relationship between the meteorological elements and the power is shown below.

Fig. 3 indicated the fluctuation trend of wind speed curve is not close to that of output power curve. And the fluctuation of wind speed curve is greater. In practical applications, the dust on the PV panels will affect the conversion efficiency of the PV system, higher wind speed can remove non-cohesive dust from PV panels, which can improve power output (Jaszczur et al., 2019; Styszko et al., 2019; Hernandez et al., 2019). There is little correlation between

Please cite this article as: Liu, Z.-F et al., Prediction short-term photovoltaic power using improved chicken swarm optimizer - Extreme learning machine model, Journal of Cleaner Production, https://doi.org/10.1016/j.jclepro.2019.119272

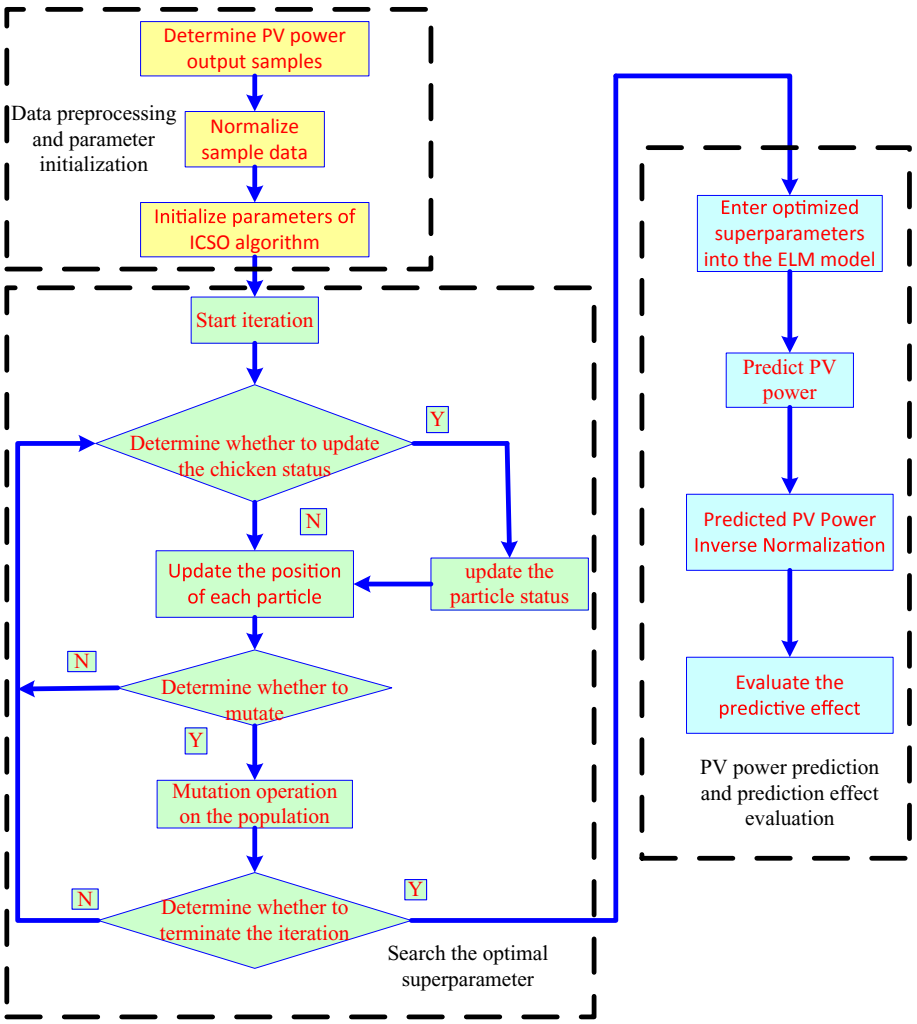

Fig. 1. The optimization process of ICSO.

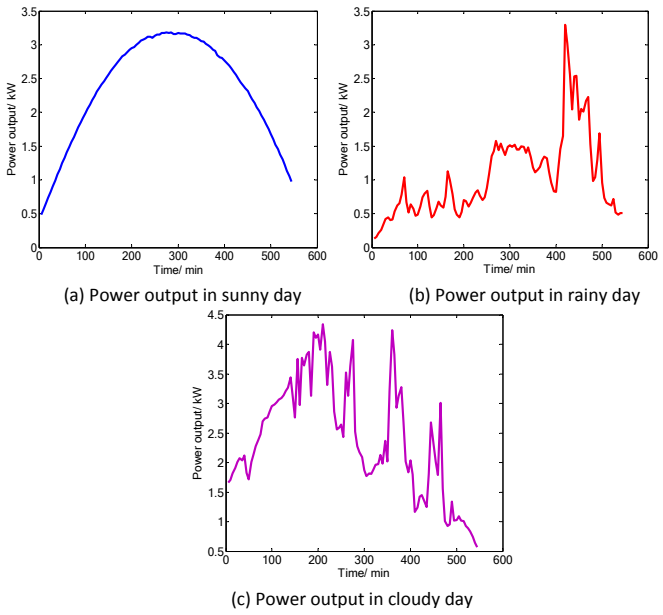

Fig. 2. The PV power output curves.

temperature and power. The relative humidity and power show a negative correlation, while the relative humidity decreases with the increase of output power. The illumination intensity and power show positive correlation and strong correlation. The output power increases with the increase of illumination intensity, and decreases with the decrease of illumination intensity.

The Pearson correlation coefficient β is used to calculate the influence of each meteorological element on the power.

$$\beta_{X,Y} = \frac{Q\sum XY - \sum X \sum Y}{\sqrt{Q\sum X^2 - (\sum X)^2}\sqrt{Q\sum Y^2 - (\sum Y)^2}} \tag{14}$$

When $|\beta|$ is close to 1, there is a stronger correlation between the two attributes; when $|\beta|$ is close to 0, there is a weaker correlation between the two attributes. Generally, the range of values in Table 1 is used to indicate the strength of correlation.

The correlation coefficient between output power and wind speed, temperature, relative humidity and radiation intensity are calculated. The results are showed in Table 2.

Table 2 presented the radiation intensity and power show the strongest correlation, reaching 0.9963. Two attributes are exceedingly more association according to Table 1. The relative humidity and power show a negative correlation, which is −0.1771. Temperature and output power are weakly correlated. Wind speed and power are strongly correlated.

Please cite this article as: Liu, Z.-F et al., Prediction short-term photovoltaic power using improved chicken swarm optimizer - Extreme learning machine model, Journal of Cleaner Production, https://doi.org/10.1016/j.jclepro.2019.119272

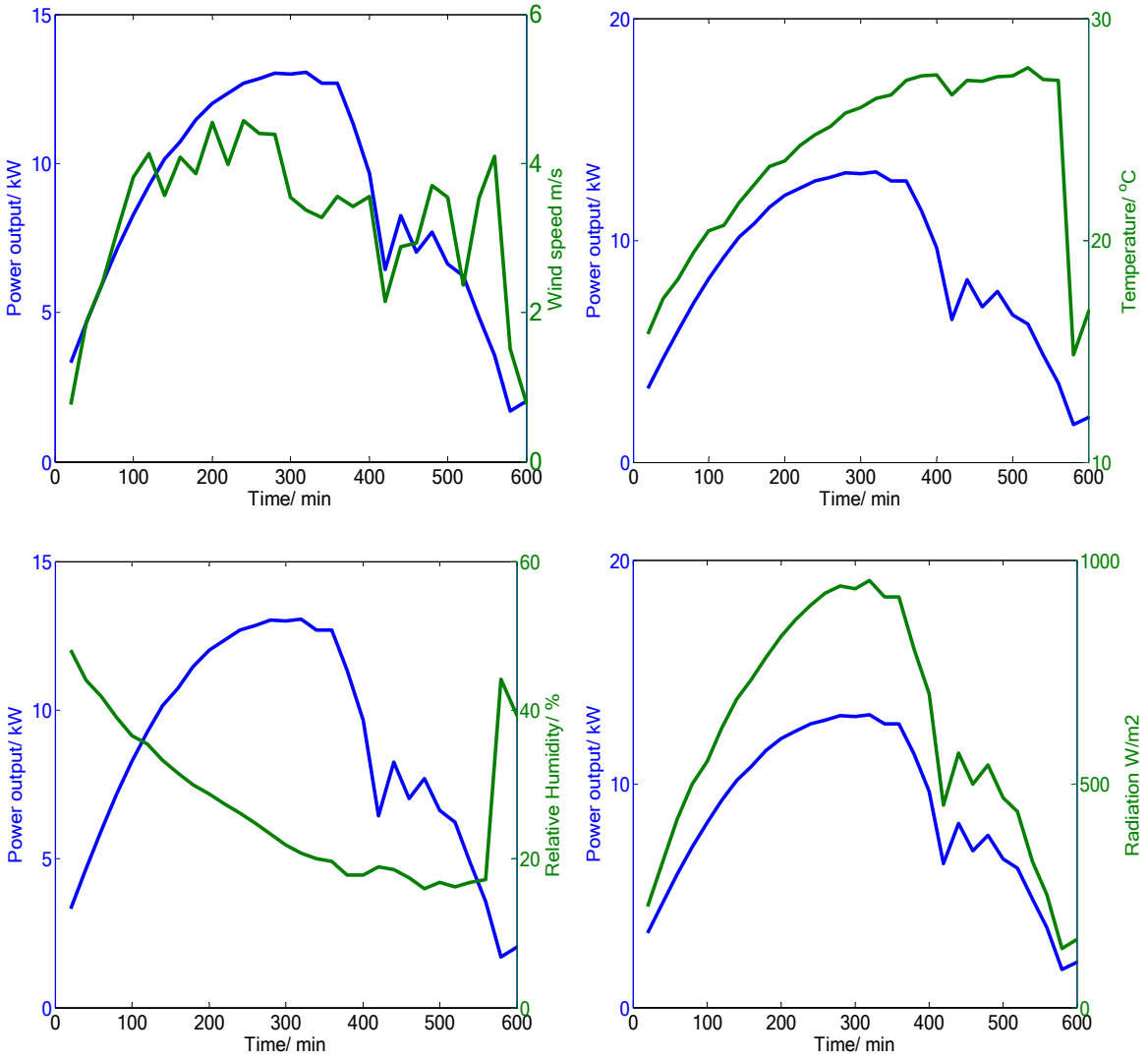

Fig. 3. Relationship curves.

Table 1
Relevant degree judgment.

$\|\beta\|$	Degree of association
0.0–0.2	Exceedingly less or no association
0.2–0.4	Less association
0.4–0.6	Moderate association
0.6–0.8	More association
0.8–1.0	Exceedingly more association

Table 2
Correlation coefficient between output power and various influencing attributes.

Attributes	β
Wind speed	0.6494
Temperature	0.2757
Relative humidity	−0.1771
Radiation intensity	0.9963

This analysis found that the temperature, radiation intensity and wind speed have great effect on the power output, and the relative humidity has little effect on the power output. Therefore, the radiation intensity, wind speed and temperature are taken as predictive model input, and the PV power is taken as predictive model output(See. Table 3).

5. Simulation experiment and experimental data analysis

5.1. Optimizer performance analysis

The test functions are used to test the optimization effect of ICSO optimizer in 30-dimensional and 100-dimensional. The optimization effects of PSO, WOA, ICSO and CSO optimizers are compared. The PSO optimizer is a classical evolutionary optimizer. Mirjalili et al. (2016) proposed the WOA optimizer. The WOA optimizer is a new bionic intelligent optimizer. All simulations in this study use unified equipment to make the experimental results more reliable.

The parameters of the four methods are as follows.

Table 4 presented the population size N of the four optimizers is 10*d (d is the dimension), and maximum number of optimizations is 500.The acceleration attributes Z_1 and Z_2 of PSO optimizer are 1.494 and the weight C is 0.729. In WOA optimizer, parameter B is used to restrict the constant coefficients in logarithmic helix form, which is taken as 1 in this study. In the CSO and ICSO optimizers, the state update interval G is 5. And cocks, hens, and chicks account

Please cite this article as: Liu, Z.-F et al., Prediction short-term photovoltaic power using improved chicken swarm optimizer - Extreme learning machine model, Journal of Cleaner Production, https://doi.org/10.1016/j.jclepro.2019.119272

Table 3
Function range and optimal value (Yang et al., 2019; Wang and Song, 2019).

M	Equations	Range	Optimum
Sphere	$M_1 = \sum_{l=1}^{m} u_l^2$	[-100, 100]	0
Schwefel	$M_2 = \sum_{l=1}^{m} \lvert u_l \rvert + \prod_{l=1}^{m} \lvert u_l \rvert$	[-10, 10]	0
Rotated hyper-ellipsoid	$M_3 = \sum_{l=1}^{m} (\sum_{j=1}^{l} u_j)^2$	[-100, 100]	0
Griewank	$M_4 = \frac{1}{4000} \sum_{l=1}^{m} u_l^2 - \prod_{l=1}^{m} \cos\left(\frac{u_l}{\sqrt{t}}\right) + 1$	[-600, 600]	0
Zakharov	$M_5 = \sum_{l=1}^{m} u_l^2 + (0.5 * \sum_{l=1}^{m} (l * u_l^2))^2 + (0.5 * \sum_{l=1}^{m} (l * u_l^2))^4$	[-100, 100]	0
Rastrigin	$M_6 = \sum_{l=1}^{m} (u_l^2 - 10 * \cos(2\pi * u_l) + 10 * m)$	[-5.12, 5.12]	0

for 30%, 50%, and 20% of the population size. The test results of the four methods are shown as Table 5.

The running speed of PSO program is the fastest among the four optimizers, and each optimization takes the least time. However, by comparison, it is found that the convergence effect of PSO optimizer is poor. For six test functions, PSO does not converge to the global optimum, whether in 30 or 100 dimensions. The analysis results show that the optimization effects of PSO and CSO optimizers become worse with the increase of dimension of standard test function, which indicates that the convergence stability of CSO and PSO optimizers is poor. The WOA optimizer converges to the global optimal value for M_4 and M_6.

Table 4
Parameters of PSO, WOA, CSO and ICSO.

Method	Setting parameters
PSO	N = 10*d, T = 500, $Z_1 = Z_2 = 1.494$,C = 0.729
WOA	N = 10*d, T = 500,B = 1
CSO	N = 10*d, T = 500,G = 5, N_r = 0.3*N, N_h = 0.5*N, N_c = 0.2*N
ICSO	N = 10*d, T = 500,G = 5, N_r = 0.3*N, N_h = 0.5*N, N_c = 0.2*N

The optimization effect of the WOA optimizer does not change significantly, which shows that the stability of the WOA optimizer is higher. However, with the increase of the dimension, the computational cost of the WOA optimizer increases significantly. At 100 dimensions, program running time of the WOA optimizer is almost twice that of the CSO and ICSO optimizers for the standard test functions M_1, M_2, M_4, M_5 and M_6. The running time of WOA optimizer is three times faster than the PSO optimizer for M_1, M_2, M_5 and M_6.

This analysis found that the optimization effect of ICSO optimizer is the best. For the standard test functions M_1, M_3, M_4, M_5 and M_6, the optimization results of the ICSO optimizer are all 0 in both 30-dimensional and 100-dimensional. For the standard test function M_2, in the 30-dimensional, the optimization result of the ICSO optimizer is 0; in the 100-dimensional, although the optimization result of the ICSO optimizer is not 0, the convergence accuracy is still the highest compared to the other three optimizers. When the test dimension increases, the optimization result of the ICSO optimizer does not change significantly, which indicates that the optimization stability of the ICSO optimizer is higher. By comparing the data in the table, the ICSO optimizer has the higher convergence accuracy and convergence stability.

Table 5
Comparison of optimization results.

M	Optimizer	Optimum 30d/100d	Worst value 30d/100d	Average value 30d/100d	Average running time/s 30d/100d
M_1	PSO	9.16e-06/9.78	5.66e-04/30.64	2.21e-04/19.07	11.84/40.87
	WOA	2.86e-115/5.63e-124	5.88e-109/1.81e-116	6.27e-110/1.86e-117	17.53/**1.33e + 02**
	CSO	9.94e-30/0.11	1.62e-27/35.48	2.81e-28/10.99	16.55/58.36
	ICSO	**0/0**	**0/0**	**0/0**	19.37/67.41
M_2	PSO	0.63/15.29	2.16/20.22	1.57/18.23	12.43/42.62
	WOA	1.93e-66/3.59e-69	2.23e-62/2.51e-64	3.56e-63/5.73e-65	23.13/**1.72e + 02**
	CSO	7.35e-23/3.87e-15	3.75e-22/1.49e-08	1.90e-22/6.21e-09	17.35/60.71
	ICSO	**0/2.00e-323**	**0/3.26e-320**	**0/6.97e-321**	20.47/73.18
M_3	PSO	16.21/1.31e+03	86.23/5.48e+03	40.60/2.33e+03	39.05/340.64
	WOA	9.68e+02/2.00e+05	1.01e+04/4.02e+05	4.61e+03/2.93e+05	48.07/**4.62e + 02**
	CSO	15.50/9.27e+02	335.77/1.65e+03	181.12/1.30e+03	37.27/2.82e+02
	ICSO	**0/0**	**0/0**	**0/0**	48.89/4.23e+02
M_4	PSO	1.71e-04/1.17	0.06/1.47	0.02/1.28	14.48/53.10
	WOA	**0/0**	**0/0**	**0/0**	20.24/**1.52e + 02**
	CSO	**0**/0.09	**0**/0.85	**0**/0.42	19.63/69.72
	ICSO	**0/0**	**0/0**	**0/0**	18.31/83.49
M_5	PSO	1.33e-04/46.97	0.14/136.93	0.02/79.73	15.48/53.65
	WOA	1.33e-39/5.11e+03	1.16e-25/1.53e+04	1.18e-26/1.16e+04	19.72/**142.24**
	CSO	1.16e-21/78.50	1.17e-19/2.06e+02	2.68e-20/1.37e+02	18.63/82.03
	ICSO	**0/0**	**0/0**	**0/0**	21.84/80.18
M_6	PSO	21.88/135.26	69.64/296.97	48.55/208.18	13.32/48.46
	WOA	**0/0**	**0/0**	**0/0**	17.88/**1.35e + 02**
	CSO	**0**/2.22e-05	**0**/4.74e-04	**0**/1.82e-04	16.41/59.82
	ICSO	**0/0**	**0/0**	**0/0**	19.12/68.05

Please cite this article as: Liu, Z.-F et al., Prediction short-term photovoltaic power using improved chicken swarm optimizer - Extreme learning machine model, Journal of Cleaner Production, https://doi.org/10.1016/j.jclepro.2019.119272

5.2. Prediction of short-term photovoltaic power output under different weather conditions

The output power of PV system is different due to different weather conditions. Three experimental samples from DKASC are used in this study. The study period of the output power is from 8:00 to 17:00. Statistics are taken every 5 min.

The PV power is predicted by the ICSO-ELM prediction model. At the same time, classic models such as BP neural network, support vector machine (SVM) and Gaussian process regression (GPR) model are used as comparison models.

The mean absolute percentage error (MAPE) and root mean square error (RMSE) are used to evaluate the prediction effect of prediction models. Decision coefficient (R^2) is used to judge the fitting degree.

$$RMSE = \sqrt{\frac{\sum_{i=1}^{M}\left(\hat{g_i} - g_i\right)^2}{M}} \tag{15}$$

$$MAPE = \frac{1}{M}\left(\sum_{i=1}^{M}\frac{|\hat{g_i} - g_i|}{g_i} * 100\right) \tag{16}$$

$$R^2 = \frac{(M\sum g\hat{g} - \sum \hat{g}\sum g)^2}{\left(M\sum\left(\hat{g_i}\right)^2 - \left(\hat{g_i}\right)^2\right)(M\sum(g)^2 - \sum(g)^2)} \tag{17}$$

where the actual value is g and the predicted value is $\hat{g}$.

The decision coefficient R^2 of the model is a very common statistical information in regression analysis. The lower bound of R^2 is 0 and the upper bound is 1. When the decision coefficient R^2 is 0, the model is completely unpredictable. When the decision coefficient R^2 is 1, the model can perfectly predict the target variable.

Firstly, the ICSO-ELM model is tested by using the sunny weather power output data during 2016.10.9–13. The power output data of 2016.10.9–12 is selected as the training set, and the PV power of 2016.10.13 is used as the test sample. The prediction results of the ICSO-ELM, CSO-ELM, BP, SVM and GPR models are shown in Fig. 4.

The prediction curves of power output of the ICSO-ELM, CSO-ELM, BP, SVM and GPR models for the sunny weather during

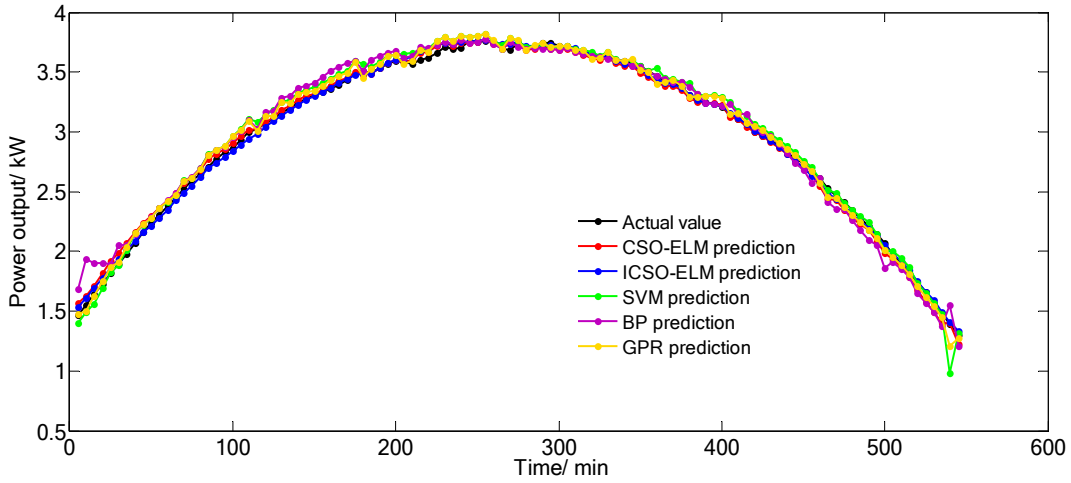

(a) Predicted power output curves on sunny day

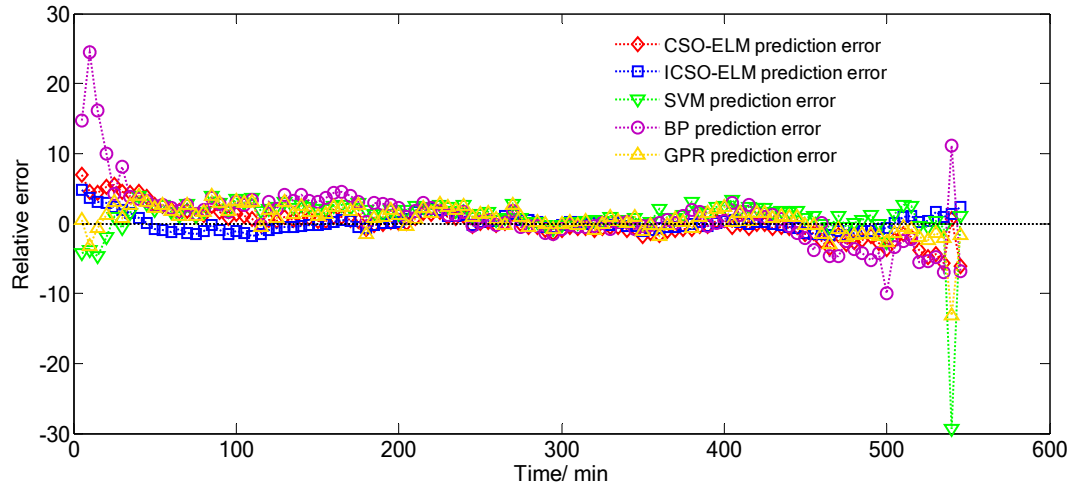

(b) Prediction relative error on sunny day

Fig. 4. Prediction results on sunny days.

Please cite this article as: Liu, Z.-F et al., Prediction short-term photovoltaic power using improved chicken swarm optimizer - Extreme learning machine model, Journal of Cleaner Production, https://doi.org/10.1016/j.jclepro.2019.119272

2016.10.10–16 are presented in Fig. 4 (a). The prediction curves of the five models can basically reflect the changing trend of the PV power curve. Analysis of the data in Fig. 4 (b) shows that the prediction error of the BP model in the early stage of prediction is larger, and the relative error exceeds 20%; the prediction errors of the four other models in the prediction medium are controlled at [-10%, 10%]; the prediction errors of the BP, GPR and SVM models at the end of the forecast fluctuate greatly, and the prediction error of the SVM model is nearly 30%.

The relative error histograms are obtained to more clearly analysis the magnitude of the prediction errors of the five prediction models, showed in Fig. 5.

Fig. 5 showed the interval distribution of the relative errors of the five prediction models. The prediction relative errors of the CSO-ELM model and the ICSO-ELM model are mainly distributed in the [-2%, 2%]. The relative error values of CSO-ELM model and ICSO-ELM model in the [-2%, 2%] account for 85.18% and 91.66% of the total test samples. The prediction relative errors of the SVM model, the BP model and the GPR model are mainly distributed in the [-5%, 5%]. The relative error values of SVM model, BP model and GPR model in the [-2%, 2%] account for 59.63%, 47.71% and 72.47% of the total test samples. Through error interval analysis, it is found that the prediction errors of CSO-ELM and ICSO-ELM models are lower.

Secondly, the ICSO-ELM model is tested by using the cloudy weather during 2016.11.27–2016.12.01. The power output data during cloudy weather of 2016.11.27–2016.11.30 is selected as the training set, and the power data from 2016.12.01 is used as the test sample. The test results of the CSO-ELM, ICSO-ELM, SVM, BP and GPR models are shown in Fig. 6.

This study finds the prediction errors of SVM, BP and GPR models are large in the early stage of prediction by comparing the predictive curves in Fig. 6 (a). The fitting effect of the predictive curves of the five models and the actual power output curve in the middle stage of prediction is higher, and the predictive curves of BP and GPR models in the late stage of prediction deviate from the true value curves. Through analysis, it is found that the prediction curve of the ICSO-ELM model can still reflect the trend of the actual power output curve in cloudy weather. The prediction errors in Fig. 6(b) increase significantly compared with the relative error values in Fig. 4(b). In the later stage of prediction, the forecasting errors of GPR model and BP model increase significantly, and the maximum prediction error of GPR model exceeds 100%, indicating that the model's prediction stability is poor for cloudy weather.

Fig. 7 shows the distribution histogram of the relative errors of the five models in cloudy weather.

The result found that the prediction error intervals of the five models in Fig. 7 increased compared with the histogram in Fig. 5. The relative error values of CSO-ELM, ICSO-ELM, SVM, BP and GPR models in the [-2%, 2%] account for 39.44%, 51.37%, 22.93%, 17.43% and 10.09% of the total test samples. The number of relative error values predicted by the five models in the range of [-2%, 2%] further decrease. Compared with the proportion of the relative error in the interval [-2%, 2%] in Fig. 5, the proportion of the relative error in the interval [-2%, 2%] in Fig. 5 is reduced by 45.74%, 40.29%, 36.70%,

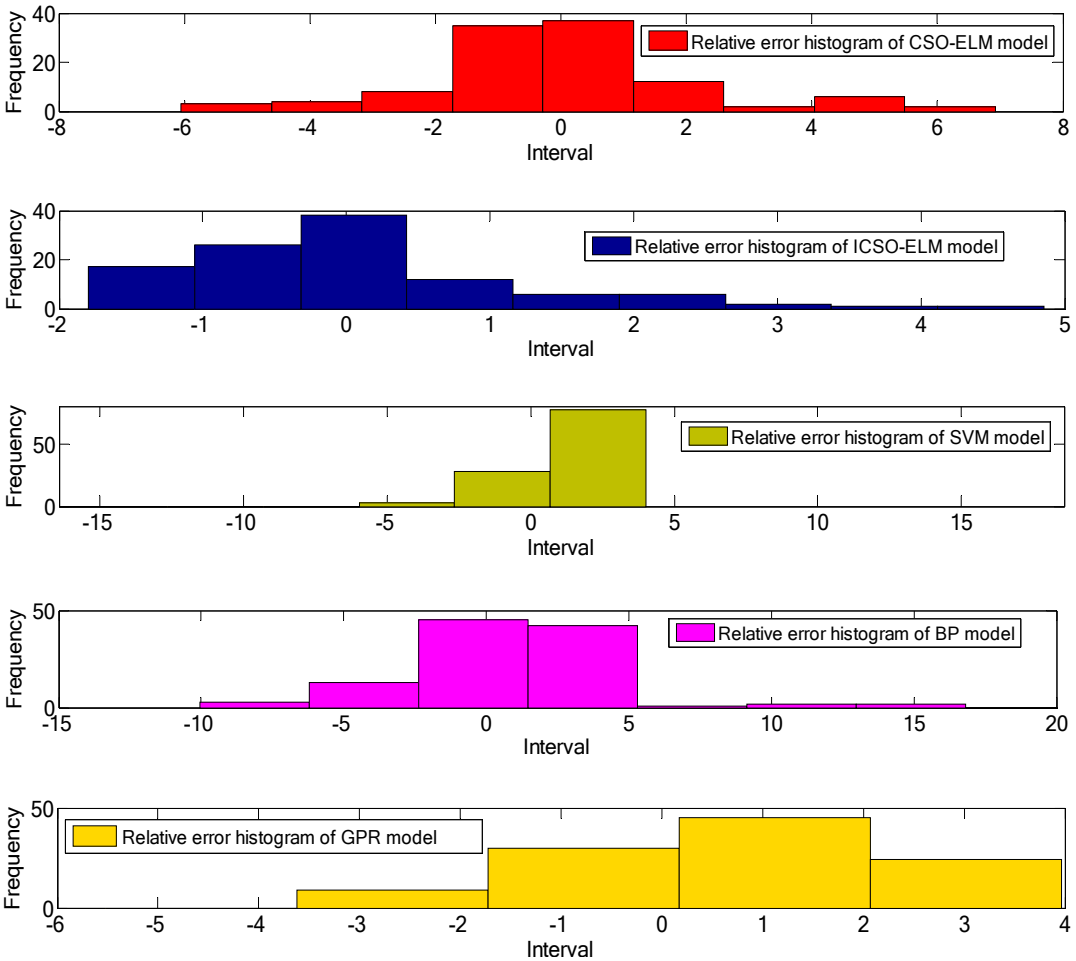

Fig. 5. Relative error histograms on sunny days.

Please cite this article as: Liu, Z.-F et al., Prediction short-term photovoltaic power using improved chicken swarm optimizer - Extreme learning machine model, Journal of Cleaner Production, https://doi.org/10.1016/j.jclepro.2019.119272

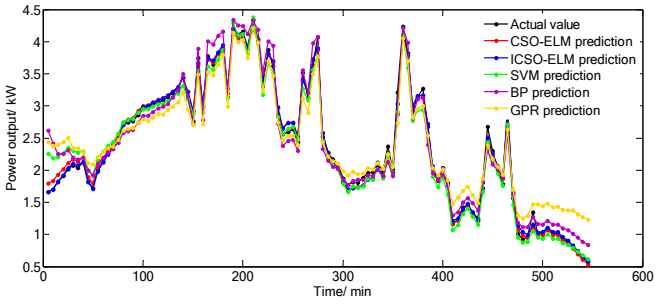

(a) Predicted power output curves on cloudy day

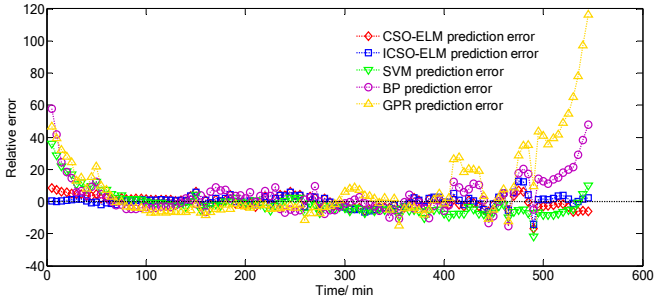

(b) Prediction relative error on cloudy day

Fig. 6. Prediction results on cloudy days.

30.28% and 62.38%. This is due to the quasi-periodic characteristics of PV power in clear weather, and the irregularity of power output in cloudy weather increases. It shows that compared with the prediction errors in sunny weather, the prediction errors of the models in cloudy weather increase.

Finally, the ICSO-ELM model is tested by using the rainy weather during 2016.9.24–28. The power output data during rainy weather of 2016.9.24–27 is selected as the training set, and the power data from 2016.9.28 is used as the test set. The prediction curves of the CSO-ELM, ICSO-ELM, SVM, BP and GPR models are shown in Fig. 8.

The PV power output curve has the characteristics of large fluctuation during rainy days. The prediction curves of the five models basically reflect the fluctuation trend of the actual power output curve. It can be seen from the local enlargement that the fitting degree between the blue curve and the black curve is the highest. At the sixteenth sample point, the SVM, BP and GPR models have large prediction errors, which is due to the uncertainty of power output in rainy days.

Similar to cloudy weather, the prediction errors of the five models increase relatively on rainy day. In Fig. 8(b), the prediction stability of the five models is higher in the middle and late stages of prediction, but the prediction stability of the CSO-ELM, SVM, BP and GPR models is poor in the early stage of prediction. Fig. 9 shows the distribution histogram of the relative errors of the five models in rainy day.

The result found that the prediction error intervals of the five models in Fig. 9 further increased compared with the histograms in Figs. 5 and 7. The relative error values of CSO-ELM, ICSO-ELM, SVM, BP and GPR models in the [-2%, 2%] range account for 17.33%, 22.01%, 12.84%, 11.01% and 12.44% of the total test samples. The proportion of the relative error in the interval [-2%, 2%] in Fig. 9 is reduced by 22.11%, 29.36%, 10.09%, 6.42% and 2.35% compared with the proportion of the relative error in the interval [-2%, 2%] in Fig. 7. The randomness of power output in rainy weather is greater than the randomness of power output in sunny and cloudy weather. Therefore, the prediction errors of five models further increase.

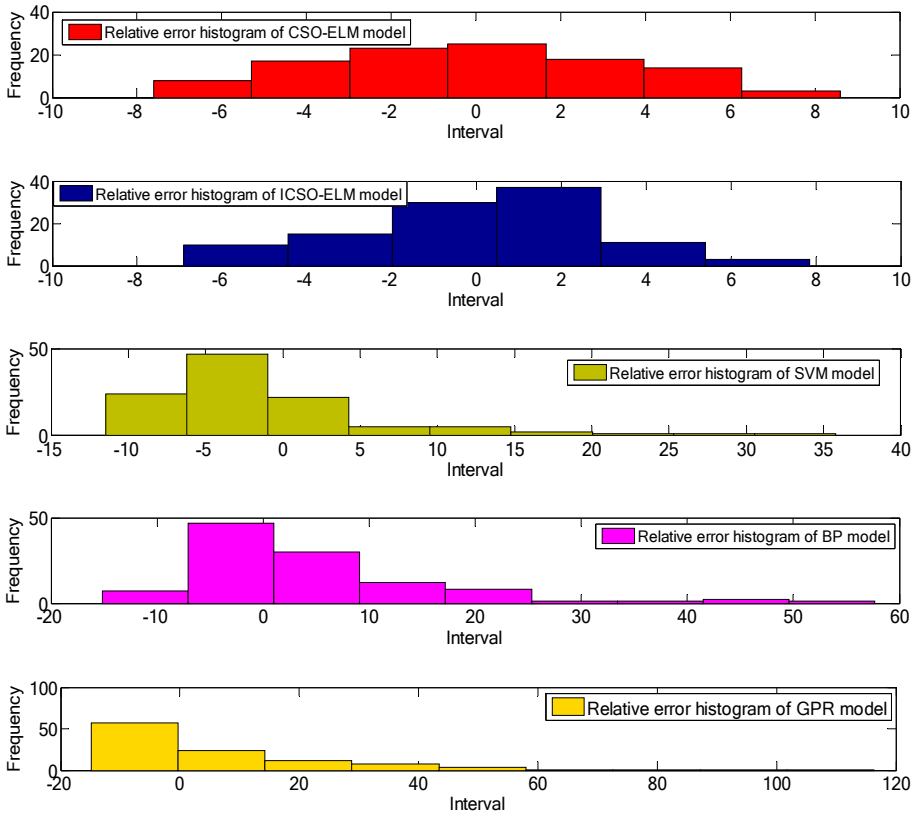

Fig. 7. Relative error percentage on cloudy days.

Please cite this article as: Liu, Z.-F et al., Prediction short-term photovoltaic power using improved chicken swarm optimizer - Extreme learning machine model, Journal of Cleaner Production, https://doi.org/10.1016/j.jclepro.2019.119272

The test results of the CSO-ELM, ICSO-ELM, SVM, BP and GPR models are assessed by evaluation indicators. The evaluation results are shown in Table 6. Table 6 compared the RMSE and MAPE values of each model in different weather conditions. Compared with sunny weather, the RMSE and MAPE obtained in rainy and cloudy weather are relatively larger. The RMSE values and the MAPE values of the ICSO-ELM model are the smallest whether it is rainy, cloudy or sunny. For three different weather conditions, the average RMSE value of CSO-ELM, ICSO-ELM, SVM, BP and GPR models are 6.51%, 5.54%, 10.83%, 13.10% and 14.35%. For three different weather conditions, the RMSE of ICSO-ELM model is the smallest, which indicates that the predictive stability of ICSO-ELM is higher.

The MAPE obtained in cloudy and rainy weather is significantly higher than the MAPE obtained in sunny weather. Because the PV power output curve has uncertainty and randomness in rainy and cloudy weather, which increases the prediction error of the model. For three different weather conditions, the average MAPE values of CSO-ELM, ICSO-ELM, SVM, BP and GPR models are 3.67%, 3.08%, 6.08%, 7.70% and 8.45%. By comparing the average MAPE of each model, it is found that the MAPE value of the ICSO-ELM model is smaller, indicating that the ICSO-ELM model maintains high prediction accuracy under three weather conditions.

For the evaluation index R^2, the R^2 obtained in sunny weather is significantly higher than the R^2 in cloudy weather and rainy weather. For three different weather conditions, the average R^2 of CSO-ELM, ICSO-ELM, SVM, BP and GPR models are 99.13%, 99.32%, 98.59%, 97.72% and 97.78%. The R^2 of the ICSO-ELM model is higher than the other four models, indicating that the ICSO-ELM model has a strong fitting effect on the output power under three different weather conditions.

6. Concluding remarks

In order to reduce the PV power curtailment rate and realize the economic dispatch of the power system, improving the accuracy of short-term PV power output prediction is an urgent subject to be studied. Therefore, the ICSO-ELM is modeled to forecast PV power in this study. The test results show that the prediction effect of ICSO-ELM model is better than CSO-ELM, SVM, BP and GPR model. And the main contributions of this study are as follows:

(1) The ICSO-ELM model is firstly proposed to predict the short-term photovoltaic power.

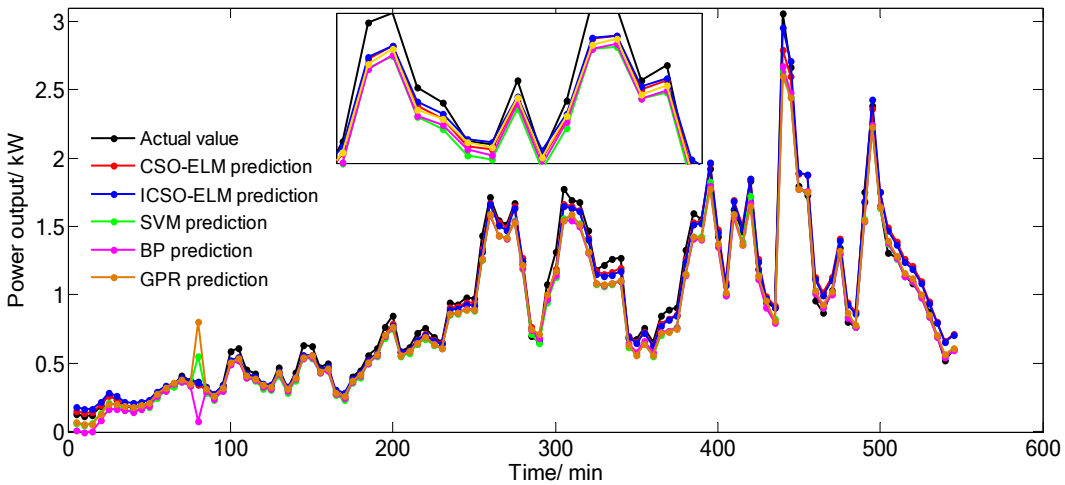

(a) Predicted power output curves on rainy day

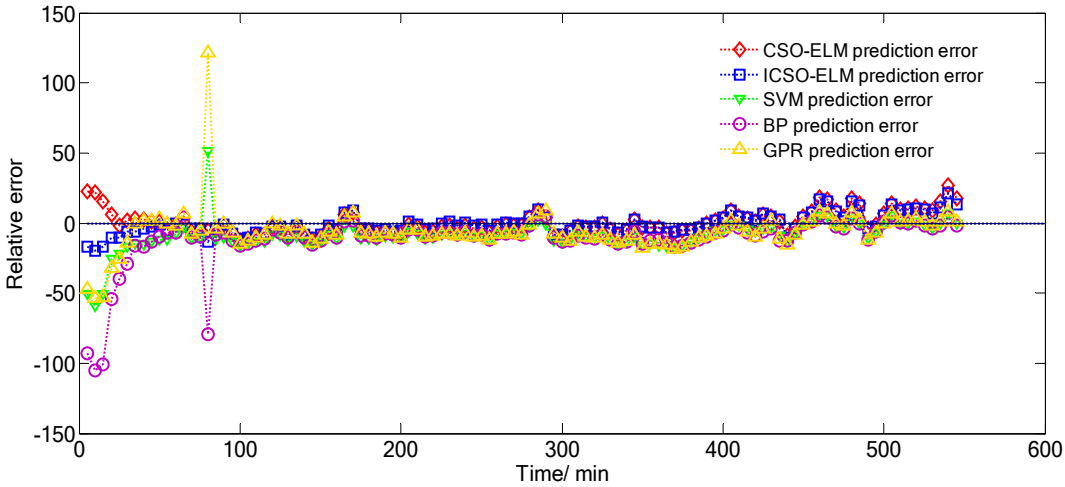

(b) Prediction relative error on rainy day

Fig. 8. Prediction results on rainy day.

Please cite this article as: Liu, Z.-F et al., Prediction short-term photovoltaic power using improved chicken swarm optimizer - Extreme learning machine model, Journal of Cleaner Production, https://doi.org/10.1016/j.jclepro.2019.119272

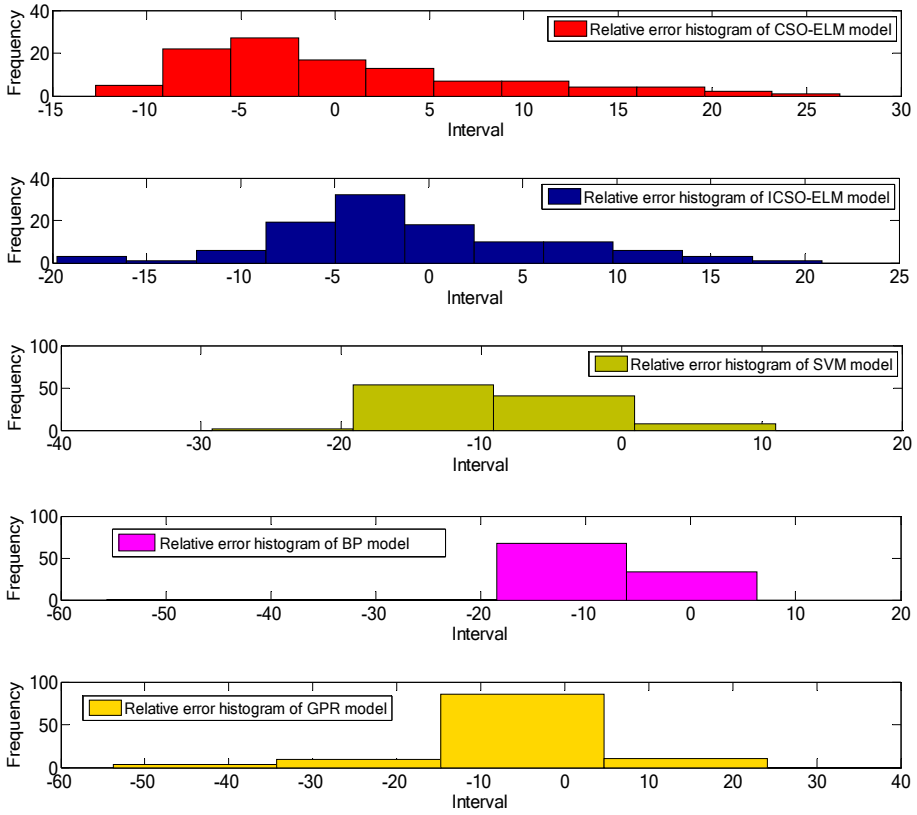

Fig. 9. Relative error percentage on rainy days.

(2) The operating and management efficiency of photovoltaic power station can be improved by accurate prediction of photovoltaic power.
(3) For three different weather conditions, the average RMSE value and the average MAPE value of ICSO-ELM model are 5.54% and 3.08%. The average MAPE values of CSO-ELM, ICSO-ELM, SVM, BP and GPR models are 3.67%, 3.08%, 6.08%, 7.70% and 8.45%; the average MAPE values of CSO-ELM, ICSO-ELM, SVM, BP and GPR models are 3.67%, 3.08%, 6.08%, 7.70% and 8.45%. The result indicates that the ICSO-ELM model has a better forecasting effect.
(4) The operating and management efficiency of photovoltaic power station can be improved by accurate prediction of photovoltaic power. And by accurately predicting PV power, the measures of abandoning solar can be reduced and the development of clean energy can be promoted.

Table 6
Evaluation of the prediction effects of five models.

Weather	Model	RMSE/%	MAPE/%	R^2/%
Sunny weather	CSO-ELM	4.43	1.51	99.61
	ICSO-ELM	**2.84**	**0.85**	**99.84**
	SVM	6.96	1.93	99.48
	BP	9.01	2.86	98.59
	GPR	5.24	1.57	99.62
Cloudy weather	CSO-ELM	8.06	3.09	99.30
	ICSO-ELM	**7.19**	**2.51**	**99.45**
	SVM	15.58	5.76	97.55
	BP	20.06	8.10	95.90
	GPR	27.12	13.93	95.97
Rainy weather	CSO-ELM	7.04	6.42	98.50
	ICSO-ELM	**6.60**	**5.89**	98.68
	SVM	9.94	10.54	**98.76**
	BP	10.24	12.15	98.66
	GPR	10.71	9.85	97.94

Although this study predicts the short-term PV power under three weather conditions, there are still many extreme weather conditions (such as haze, ice and snow) that are not taken into account. In the future, we should study the PV power prediction under extreme weather conditions and improve the stability of the prediction model.

Author contribution statement

- Zhi-Feng Liu drafts this manuscript
- Ling-Ling Li structures to structure this manuscript
- Ming-Lang Tseng finalizes this manuscript
- Ming K. Lim finalizes this manuscript

Declaration of competing interest

There is none Conflicts of Interests.

Acknowledgements

This work was supported by the Natural Science Foundation of Hebei Province of China [Project No. E2018202282] and the key project of Tianjin Natural Science Foundation [Project No. 19JCZDJC32100].

References

Bacher, P., Madsen, H., Nielsen, H.A., 2009. Online short-term solar power

forecasting. Sol. Energy 83 (10), 1772–1783.
Bouzerdoum, M., Mellit, A., Pavan, A.M., 2013. A hybrid model (SARIMA-SVM) for short-term power forecasting of a small-scale grid-connected photovoltaic plant. Sol. Energy 98, 226–235.
Cervone, G., Clemente-Harding, L., Alessandrini, S., Delle Monache, L., 2017. Short-term photovoltaic power forecasting using artificial neural networks and an analog ensemble. Renew. Energy 108, 274–286.
Dolara, A., Grimaccia, F., Leva, S., Mussetta, M., Ogliari, E., 2015. A physical hybrid artificial neural network for short term forecasting of PV plant power output. Energies 8 (2), 1138–1153.
Eseye, A.T., Zhang, J.H., Zheng, D.H., 2018. Short-term photovoltaic solar power forecasting using a hybrid Wavelet-PSO-SVM model based on SCADA and Meteorological information. Renew. Energy 118, 357–367.
Guner, A., Alcin, O.F., Sengur, A., 2019. Automatic digital modulation classification using extreme learning machine with local binary pattern histogram features. Measurement 145, 214–225.
Guo, X.P., Lin, K., Huang, H., Li, Y., 2019. Carbon footprint of the photovoltaic power supply chain in China. J. Clean. Prod. 233, 626–633.
Han, S., Qiao, Y.H., Yan, J., Liu, Y.Q., Li, L., Wang, Z., 2019a. Mid-to-long Term Wind and Photovoltaic Power Generation Prediction Based on Copula Function and Long Short Term Memory Network.
Han, Y.T., Wang, N.B., Ma, M., Zhou, H., Dai, S.Y., Zhu, H.L., 2019b. A PV power interval forecasting based on seasonal model and nonparametric estimation algorithm. Sol. Energy 184, 515–526.
Hernandez, J.C., Sanchez-Sutil, F., Vidal, P.G., Rus-Casas, C., 2018. Primary frequency control and dynamic grid support for vehicle-to-grid in transmission systems. Int. J. Electr. Power Energy Syst. 100, 152–166.
Hernandez, J.C., Sanchez-Sutil, F., Munoz-Rodriguez, F.J., 2019. Design criteria for the optimal sizing of a hybrid energy storage system in PV household-prosumers to maximize self-consumption and self-sufficiency. Energy 186.
Hossain, M., Mekhilef, S., Danesh, M., Olatomiwa, L., Shamshirband, S., 2017. Application of extreme learning machine for short term output power forecasting of three grid-connected PV systems. J. Clean. Prod. 167, 395–405.
Huang, G.B., Zhu, Q.Y., Siew, C.K., 2006. Extreme learning machine: theory and applications. Neurocomputing 70 (1–3), 489–501.
Izgi, E., Oztopal, A., Yerli, B., Kaymak, M.K., Sahin, A.D., 2012. Short-mid-term solar power prediction by using artificial neural networks. Sol. Energy 86 (2), 725–733.
Jaszczur, M., Teneta, J., Styszko, K., Hassan, Q., Burzynska, P., Marcinek, E., Lopian, N., 2019. The field experiments and model of the natural dust deposition effects on photovoltaic module efficiency. Environ. Sci. Pollut. Control Ser. 26 (9), 8402–8417.
Li, Y.T., Su, Y., Shu, L.J., 2014. An ARMAX model for forecasting the power output of a grid connected photovoltaic system. Renew. Energy 66, 78–89.
Li, C.B., Lin, S.S., Xu, F.Q., Liu, D., Liu, J.C., 2018. Short-term wind power prediction based on data mining technology and improved support vector machine method: a case study in Northwest China. J. Clean. Prod. 205, 909–922.
Li, L.L., Wen, S.Y., Tseng, M.L., Wang, C.S., 2019a. Renewable energy prediction: a novel short-term prediction model of photovoltaic output power. J. Clean. Prod. 228, 359–375.
Li, L.L., Sun, J., Tseng, M.L., Li, Z.G., 2019b. Extreme learning machine optimized by whale optimization algorithm using insulated gate bipolar transistor module aging degree evaluation. Expert Syst. Appl. 127, 58–67.
Lin, K.P., Pai, P.F., 2016. Solar power output forecasting using evolutionary seasonal decomposition least-square support vector regression. J. Clean. Prod. 134, 456–462.
Lin, P.J., Peng, Z.N., Lai, Y.F., Cheng, S.Y., Chen, Z.C., Wu, L.J., 2018. Short-term power prediction for photovoltaic power plants using a hybrid improved Kmeans-GRA-Elman model based on multivariate meteorological factors and historical power datasets. Energy Convers. Manag. 177, 704–717.
Liu, L.Y., Zhao, Y., Chang, D.L., Xie, J.Y., Ma, Z.Y., Sun, Q., et al., 2018. Prediction of short-term PV power output and uncertainty analysis. Appl. Energy 228, 700–711.
Menezes, E.J.N., Araujo, A.M., da Silva, N.S.B., 2018. A review on wind turbine control and its associated methods. J. Clean. Prod. 174, 945–953.
Meng, X.B., Liu, Y., Gao, X.Z., Zhang, H.Z., 2014. A new bio-inspired algorithm: chicken swarm optimization. In: Tan, Y., Shi, Y., Coello, C.A.C. (Eds.), Advances in Swarm Intelligence, vol. 8794, pp. 86–94.
Mirjalili, S., Lewis, A., 2016. The whale optimization algorithm. Adv. Eng. Software 95, 51–67.
Monfared, M., Fazeli, M., Lewis, R., Searle, J., 2019. Fuzzy predictor with additive learning for very short-term PV power generation. Ieee Access 7, 91183–91192.
Nespoli, A., Ogliari, E., Leva, S., Pavan, A.M., Mellit, A., Lughi, V., Dolara, A., 2019. Day-ahead photovoltaic forecasting: a comparison of the most effective techniques. Energies 12 (9), 15.
Ni, Q., Zhuang, S.X., Sheng, H.M., Kang, G.Q., Xiao, J., 2017. An ensemble prediction intervals approach for short-term PV power forecasting. Sol. Energy 155, 1072–1083.
Raza, M.Q., Nadarajah, M., Ekanayake, C., 2016. On recent advances in PV output power forecast. Sol. Energy 136, 125–144.
Sanchez-Sutil, F., Cano-Ortega, A., Hernandez, J.C., Rus-Casas, C., 2019. Development and calibration of an open source, low-cost power smart meter prototype for PV household-prosumers. Electronics 8 (8), 29.
Seyedmahmoudian, M., Jamei, E., Thirunavukkarasu, G.S., Soon, T.K., Mortimer, M., Horan, B., et al., 2018. Short-term forecasting of the output power of a building-integrated photovoltaic system using a Metaheuristic approach. Energies 11 (5), 23.
Shi, W.G., Guo, Y., Yan, S.X., Yu, Y., Luo, P., Li, J.X., 2018. Optimizing directional reader antennas deployment in Uhf rfid localization system by using a mpcso algorithm. IEEE Sens. J. 18 (12), 5035–5048.
Styszko, K., Jaszczur, M., Teneta, J., Hassan, Q., Burzynska, P., Marcinek, E., et al., 2019. An analysis of the dust deposition on solar photovoltaic modules. Environ. Sci. Pollut. Control Ser. 26 (9), 8393–8401.
VanDeventer, W., Jamei, E., Thirunavukkarasu, G.S., Seyedmahmoudian, M., Soon, T.K., Horan, B., et al., 2019. Short-term PV power forecasting using hybrid GASVM technique. Renew. Energy 140, 367–379.
Wang, C.F., Song, W.X., 2019. A novel firefly algorithm based on gender difference and its convergence. Appl. Soft Comput. 80, 107–124.
Wang, H., Sun, J.B., Wang, W.J., 2018a. Photovoltaic power forecasting based on EEMD and a variable-weight combination forecasting model. Sustainability 10 (8), 11.
Wang, Q., Ji, S.X., Hu, M.Q., Li, W., Liu, F.S., Zhu, L., 2018b. Short-term photovoltaic power generation combination forecasting method based on similar day and cross entropy theory. Int. J. Photoenergy 10.
Wang, Y.K., Tang, H.M., Wen, T., Ma, J.W., 2019. A hybrid intelligent approach for constructing landslide displacement prediction intervals. Appl. Soft Comput. 81, 16.
Xie, T., Zhang, G., Liu, H.C., Liu, F.C., Du, P.D., 2018. A hybrid forecasting method for solar output power based on variational mode decomposition, deep belief networks and auto-regressive moving average. Appl. Sci.-Basel 8 (10), 24.
Xiong, P.P., Yan, W.J., Wang, G.Z., Pei, L.L., 2019. Grey extended prediction model based on IRLS and its application on smog pollution. Appl. Soft Comput. 80, 797–809.
Xue, X.W., Yao, M., Wu, Z.H., 2018. A novel ensemble-based wrapper method for feature selection using extreme learning machine and genetic algorithm. Knowl. Inf. Syst. 57 (2), 389–412.
Yang, B., Zhong, L.E., Zhang, X.S., Shu, H.C., Yu, T., Li, H.F., et al., 2019. Novel bio-inspired memetic salp swarm algorithm and application to MPPT for PV systems considering partial shading condition. J. Clean. Prod. 215, 1203–1222.
Zhang, K., Dong, J., Huang, L.Y., Xie, H.Q., 2019. China's carbon dioxide emissions: an interprovincial comparative analysis of foreign capital and domestic capital. J. Clean. Prod. 237, 12.
Zhu, H.L., Lian, W.W., Lu, L.X., Dai, S.Y., Hu, Y., 2017. An improved forecasting method for photovoltaic power based on adaptive BP neural network with a scrolling time window. Energies 10 (10), 18.

Please cite this article as: Liu, Z.-F et al., Prediction short-term photovoltaic power using improved chicken swarm optimizer - Extreme learning machine model, Journal of Cleaner Production, https://doi.org/10.1016/j.jclepro.2019.119272